FULL PAPER

Dalton
www.rsc.org/dalton

Synthesis, structure and magnetic properties of hydroxyquinaldine-bridged cobalt and nickel cubanes

Guillem Aromí,[a] Andrei S. Batsanov,[b] Paul Christian,[a] Madeleine Helliwell,[a] Olivier Roubeau,[c] Grigore A. Timco[d] and Richard E. P. Winpenny*[a]

[a] *Department of Chemistry, The University of Manchester, Oxford Road, Manchester, UK M13 9PL. E-mail: richard.winpenny@man.ac.uk*

[b] *Department of Chemistry, The University of Durham, South Road, Durham, UK DH1 3LE*

[c] *Centre de Recherche Paul Pascal, 115 avenue du Dr Schweitzer, 33600 Pessac, France*

[d] *Institute of Chemistry, Moldovan Academy of Sciences, Academy Strasse 3, Chisinau, MD-2028, Republic of Moldova*

Received 5th August 2003, Accepted 15th September 2003
First published as an Advance Article on the web 30th September 2003

Nickel and cobalt heterocubanes have been synthesised from dinuclear complexes. The use of 8-hydroxyquinaldine leads to a rhombohedral distortion in two faces of the cubes. Both cubes were studied by paramagnetic NMR, which shows that they are stable in solution. Magnetic measurements show that the coupling within both molecules is overall antiferromagnetic. The magnetic data for the nickel cube has been modelled, and shows that the coupling consists of two ferromagnetically coupled pairs which are antiferromagnetically coupled to give a diamagnetic ground state.

Introduction

There is great interest in the synthesis and study of heterocubanes featuring the first row transition metals.[1] Initially this was led by studies into biological systems, *e.g.* models for Fe_4S_4 electron transfer sites,[2] or for the oxygen-evolving complex in PSII.[3] In more recent times the motif has drawn interest from groups studying magnetic systems. It has been suggested[4] that these cubanes offer a way to model, and so better understand, the properties of extended networks that are often based on a cubane repeat unit. Several Co and Ni cubanes have already been published in the literature, and their magnetic properties studied.[1,4,5] These results suggest that with the correct geometry ferromagnetic coupling between the metal centres can be found. We were therefore interested in extending this family of cages.

In this paper we report the synthesis and magnetic properties of isostructural Ni(II) and Co(II) cubanes. These compounds contain the 8-hydroxyquinaldine (Mq) ligand (Scheme 1). Whilst 8-hydroxyquinoline has been used for the synthesis of large transition metal clusters[6] the use of 8-hydroxyquinaldine in this context has been more restricted; this is probably due to its tendency to form mononuclear bis[7] or tris[8] complexes. Five polynuclear complexes with Mq have been reported: an oxo-bridge iron dimer,[9] a nickel trimer,[10] two copper(I) dimers[11] and a copper(I) tetramer.[12]

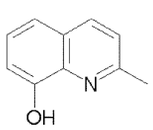

Scheme 1 8-Hydroxyquinaldine (2-methyl-8-hydroxyquinoline).

Experimental

8-Hydroxyquinaldine, pivalic acid (Hpiv) and cobalt carbonate were obtained from Aldrich and used as received. $[Co_2(H_2O)(Piv)_4(HPiv)_4]$ **1** and $Ni_2(H_2O)(Piv)_4(HPiv)_4$ **2** were made by literature methods, in which the respective metal carbonate is heated in excess pivalic acid to 100 °C, before cooling and extraction with MeCN.[13] Analytical data were obtained by the microanalytical service of the University of Manchester. Mass spectra were obtained by electrospray techniques on a Hewlett Packard 5890 Series II Gas Chromatographer coupled to a Fisons Instruments VG TRIO spectrometer spectrometer, using a 30 V cone voltage in MeCN as the carrier phase. UV-Vis spectra were recorded on a double beam Cary Varian 500 scan spectrophotometer. FT-IR spectra were recorded on a Perkin Elmer Spectrum RXI spectrometer. 300 MHz ^{1}H NMR spectra were measured on a Varian Unity Inova 300 instrument.

Preparation of samples

$[Co_4(Piv)_4(Mq)_4]$ 3. Complex **1** (2.2 g, 2.3 mmol) was dissolved in acetone (50 ml) and a solution of 8-hydroxyquinaldine (Mq) (0.73 g, 4.6 mmol) in acetone (10 ml) was added. The solution changed colour from deep blue to deep red. Red hexagonal crystals suitable for X-ray diffraction were obtained after standing for 3 days. Yield: 65.3%. Found: Co, 17.7; C, 56.8; H, 5.53; N, 4.36. Calc.: Co, 18.5; C, 56.6; H, 5.38; N, 4.40%. Mass spectrum (positive ion, ES-MS): *m*/*z* 1171, $Co_4(Piv)_3(Mq)_4$; 1114, $Co_4(Piv)_4(Mq)_3$; IR (Nujol, ν_{max}/cm^{-1}): 1598, (Ar–H); 1572 & 1553, (C=O); UV-Vis (CH_2Cl_2): λ_{max}/nm (ε_{max}/M^{-1} cm^{-1}): 1248 (19), 570 (19), 520 (19), 470 (19), 355 (28626).

$[Ni_4(Piv)_4(Mq)_4]$ 4. Complex **2** (2.41 g, 2.5 mmol) was dissolved in acetone (50 ml) and a solution of 8-hydroxyquinaldine (Mq) (0.84 g, 5.3 mmol) in acetone (10 ml) was added. The solution darkened a little upon the addition of Mq. Green hexagonal crystals suitable for X-ray diffraction were obtained after standing for 3 days. Yield: 46%. Found: Ni, 17.7; C, 56.6; H, 5.53; N, 4.31. Calc.: Ni, 17.8; C, 58.2; H, 5.19; N 4.24%. Mass spectum (positive ion, ES-MS): *m*/*z* 1169, $Ni_4(Piv)_3(Mq)_4$; IR (Nujol, ν_{max}/cm^{-1}): 3500, (O–H); 1598, (Ar–H); 1572 and 1553, (C=O); UV-Vis (CH_2Cl_2): λ_{max}/nm (ε_{max}/M^{-1} cm^{-1}): 1248 (10), 671 (10), 345 (28626).

Crystallography

Crystal data and data collection and refinement parameters for compounds **3** and **4** are given in Table 1, selected bond lengths and angles in Tables 2 and 3.

Data collection and processing

Data were collected using graphite-monochromated Mo-Kα radiation. Data for **3** were collected on a Bruker Apex diffractometer using ω scans while data for **4** were collected on a

DOI: 10.1039/b309325e

Table 1 Crystal and structural refinement for **3** and **4**

	3	**4**
Formula	$C_{60}H_{68}N_4O_{12}Co_4 \cdot 0.5C_3H_6O$	$C_{60}H_{68}N_4O_{12}Ni_4 \cdot 0.5H_2O \cdot 0.25C_2H_3O$
M_w	1301.9	1294.8
Crystal system	Monoclinic	Monoclinic
Space group	$P2_1/c$	$P2_1/c$
a/Å	15.798(5)	15.774(1)
b/Å	13.933(4)	13.955(1)
c/Å	27.648(7)	27.3512(3)
β/°	99.19(1)	98.98(1)
V/Å^3	6008(3)	5946.8(9)
Z	4	4
T/K	120(2)	100(2)
μ(Mo-Kα)/mm^{-1}	1.15	1.313
No. unique data	15916	10380
No. data with $I > 2\sigma(I)$	12671	9207
R_1, wR_2	0.0391, 0.0932	0.0313, 0.0835

Table 2 Selected bond lengths (Å)

	3	**4**
M(1)–O(1)	2.091(2)	2.042(2)
M(1)–O(3)	2.181(2)	2.124(2)
M(1)–O(4)	2.150(2)	2.079(2)
M(1)–O(5)	2.091(2)	2.068(2)
M(1)–O(12)	2.016(2)	2.015(2)
M(1)–N(1)	2.150(2)	2.102(2)
M(2)–O(1)	2.130(2)	2.058(2)
M(2)–O(2)	2.085(2)	2.051(2)
M(2)–O(4)	2.192(2)	2.134(2)
M(2)–O(6)	2.004(2)	2.004(2)
M(2)–O(7)	2.100(2)	2.077(2)
M(2)–N(2)	2.144(2)	2.089(2)
M(3)–O(1)	2.175(2)	2.125(2)
M(3)–O(2)	2.164(2)	2.083(2)
M(3)–O(3)	2.080(2)	2.043(2)
M(3)–O(8)	1.999(2)	1.993(2)
M(3)–O(9)	2.064(2)	2.050(2)
M(3)–N(3)	2.150(2)	2.097(2)
M(4)–O(2)	2.164(2)	2.113(2)
M(4)–O(3)	2.134(2)	2.060(2)
M(4)–O(4)	2.102(2)	2.060(2)
M(4)–O(10)	2.016(2)	2.017(2)
M(4)–O(11)	2.072(2)	2.059(2)
M(4)–N(4)	2.139(2)	2.088(2)
M(1)–M(2)	3.122(1)	3.032(1)
M(1)–M(3)	3.351(1)	3.242(1)
M(1)–M(4)	3.103(1)	3.013(1)
M(2)–M(3)	3.094(1)	3.006(1)
M(2)–M(4)	3.368(1)	3.269(1)
M(3)–M(4)	3.090(1)	3.001(1)

Nonius Kappa CCD using ϕ–ω scans. Both diffractometers were equipped with an Oxford Cryosystems low-temperature device.[14] Data were corrected for Lorentz and polarisation factors. Absorption corrections for **3** and **4** used SADABS[15] and SORTAV[15] respectively, giving: for **3**, T_{min} = 0.5145, T_{max} = 0.6690; for **4**, $T_{min} = T_{max}$ = 0.7792.

Structure analysis and refinement

Both structures were solved by direct methods using SHELXS-97,[15] and completed by iterative cycles of ΔF-syntheses and full-matrix least-squares refinement. All non-H atoms were refined anisotropically except atoms within disordered solvent fragments. Methyl groups were refined as rigid rotating bodies with optimised C–H distances and a common isotropic thermal parameter for the three H-atoms of each methyl. Ring H-atoms were included in idealised positions, allowed to ride on their parent C-atoms [C–H 0.93 Å], and refined with isotropic thermal parameters. All refinements were against F^2 and used SHELXL-97.[15]

CCDC reference numbers 216670 and 216671.

See http://www.rsc.org/suppdata/dt/b3/b309325e/ for crystallographic data in CIF or other electronic format.

Magnetic measurements

Field cooled measurements of the magnetisation of smoothly powdered microcrystalline samples of **3** and **4** were performed in the range 300–1.8 K with a Quantum Design MPMS-7XL SQUID magnetometer with an applied field of 1 or 10 kG. Corrections for diamagnetic contributions to the magnetic susceptibility were performed by using Pascal's constants.

Results and discussion

Structural characterisation

The two heterocubanes **3** and **4** are isostructural (Fig. 1). The $\{M_4O_4\}$ cubane contains four μ_3-oxygen atoms from Mq ligands. The faces of the cubane fall into two groups. Above two faces, that are mutually *trans*, two Mq ligands are found, with the O-atom at the corner of the cubane and the N-atom bound to a metal atom of the face. The ligands are arranged so that they point in opposite directions, and are not parallel: the angles between the mean planes of the ligands on each face are: 33.5 and 50.4° in **3** and 33.8 and 50.4° in **4**. The Mq ligands show a 4.31-bonding mode (Harris notation[16]). The remaining four faces of the cube are capped by four 2.11-bridging pivalates which lie across the face diagonals. It is interesting that attempts to synthesis the acetate bridged species from cobalt or nickel acetate only results in the formation of the bis-quinaldine complexes. This suggests that the dimeric structure

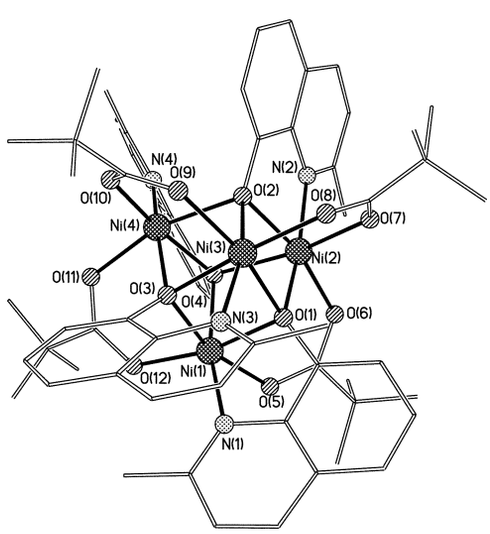

Fig. 1 Structure of **4** in the crystal; **3** is isostructural.

Table 3 Selected bond angles (°)

	3	4		3	4
O(12)–M(1)–O(1)	166.87(6)	168.08(6)	O(8)–M(3)–O(9)	105.02(7)	169.32(6)
O(12)–M(1)–O(5)	105.72(6)	102.71(6)	O(8)–M(3)–O(3)	167.61(6)	101.77(7)
O(1)–M(1)–O(5)	84.64(6)	86.00(6)	O(9)–M(3)–O(3)	85.68(6)	86.53(6)
O(12)–M(1)–O(4)	86.43(6)	86.22(6)	O(8)–M(3)–N(3)	106.90(7)	86.97(6)
O(1)–M(1)–O(4)	85.75(6)	85.89(6)	O(9)–M(3)–N(3)	88.39(7)	86.60(6)
O(5)–M(1)–O(4)	88.78(6)	88.50(6)	O(3)–M(3)–N(3)	79.18(7)	88.17(6)
O(12)–M(1)–N(1)	108.47(7)	107.65(7)	O(8)–M(3)–O(2)	87.80(6)	106.33(7)
O(1)–M(1)–N(1)	78.88(7)	80.11(7)	O(9)–M(3)–O(2)	88.35(6)	80.35(7)
O(5)–M(1)–N(1)	90.81(7)	90.21(7)	O(3)–M(3)–O(2)	86.27(6)	88.34(7)
O(4)–M(1)–N(1)	164.59(7)	165.99(7)	N(3)–M(3)–O(2)	165.29(7)	166.67(7)
O(12)–M(1)–O(3)	92.76(6)	92.68(6)	O(8)–M(3)–O(1)	92.24(6)	93.24(6)
O(1)–M(1)–O(3)	75.98(6)	77.70(6)	O(9)–M(3)–O(1)	160.81(6)	77.66(6)
O(5)–M(1)–O(3)	159.82(6)	162.74(6)	O(3)–M(3)–O(1)	76.33(6)	162.94(6)
O(4)–M(1)–O(3)	84.26(6)	84.73(6)	N(3)–M(3)–O(1)	94.65(6)	84.55(6)
N(1)–M(1)–O(3)	90.94(6)	92.53(6)	O(2)–M(3)–O(1)	83.93(6)	95.22(7)
O(6)–M(2)–O(2)	165.58(6)	166.87(6)	O(10)–M(4)–O(11)	104.66(7)	101.52(6)
O(6)–M(2)–O(7)	106.70(6)	86.04(6)	O(10)–M(4)–O(4)	167.08(7)	168.33(6)
O(2)–M(2)–O(7)	86.12(6)	87.11(6)	O(11)–M(4)–O(4)	85.94(6)	87.21(6)
O(6)–M(2)–O(1)	86.68(6)	103.77(6)	O(10)–M(4)–O(3)	86.42(7)	85.73(6)
O(2)–M(2)–O(1)	87.01(6)	87.23(6)	O(11)–M(4)–O(3)	87.87(6)	88.06(6)
O(7)–M(2)–O(1)	88.88(6)	88.57(6)	O(4)–M(4)–O(3)	86.63(6)	86.85(6)
O(6)–M(2)–N(2)	106.98(7)	106.76(7)	O(10)–M(4)–N(4)	108.65(8)	107.67(7)
O(2)–M(2)–N(2)	79.75(7)	80.71(7)	O(11)–M(4)–N(4)	84.75(7)	85.37(7)
O(7)–M(2)–N(2)	86.85(7)	167.05(7)	O(4)–M(4)–N(4)	79.24(7)	80.51(7)
O(1)–M(2)–N(2)	166.33(7)	86.48(7)	O(3)–M(4)–N(4)	164.47(7)	166.01(7)
O(6)–M(2)–O(4)	91.08(6)	91.56(6)	O(10)–M(4)–O(2)	92.94(7)	93.54(6)
O(2)–M(2)–O(4)	75.35(6)	76.59(6)	O(11)–M(4)–O(2)	160.54(6)	163.07(6)
O(7)–M(2)–O(4)	160.36(6)	84.09(6)	O(4)–M(4)–O(2)	75.61(6)	76.87(6)
O(1)–M(2)–O(4)	83.77(6)	162.51(6)	O(3)–M(4)–O(2)	84.96(6)	85.38(6)
N(2)–M(2)–O(4)	96.04(6)	97.23(6)	N(4)–M(4)–O(2)	97.60(7)	97.47(7)

Table 4 Bond angles at μ_3-O-atoms (°)

	3	4
M(1)–O(1)–M(2)	95.4(1)	95.4(1)
M(1)–O(1)–M(3)	103.5(1)	102.1(1)
M(2)–O(1)–M(3)	91.9(1)	91.9(1)
M(2)–O(2)–M(3)	93.4(1)	93.3(1)
M(2)–O(2)–M(4)	104.9(1)	103.5(1)
M(3)–O(2)–M(4)	91.1(1)	91.3(1)
M(1)–O(3)–M(3)	103.7(1)	102.1(1)
M(1)–O(3)–M(4)	92.0(1)	92.1(1)
M(3)–O(3)–M(4)	94.3(1)	94.0(1)
M(1)–O(4)–M(2)	91.9(1)	92.1(1)
M(1)–O(4)–M(4)	93.7(1)	93.4(1)
M(2)–O(4)–M(4)	103.3(1)	102.4(1)

of the starting material plays an important role in controlling the architecture of these clusters.

The magnetic superexchange is likely to be dominated by the μ_3-oxygen atoms, and a correlation between the Ni–O–Ni angle at such O-atoms and the magnetic exchange has been published.[17] The relevant structural parameters concerning these atoms are given in Table 4. The possible relationship between these parameters and the magnetic data of **4** is discussed below.

UV-Vis measurements

A solution of **3** dissolved in CH_2Cl_2 is deep red – a colour associated more frequently with cobalt(III) than cobalt(II). Therefore a closer study of the electronic spectra of **3** and **4** was carried out. UV-Vis spectra were recorded at two different concentrations so that the extinction coefficients of both the intense band at *ca.* 350 nm, and weaker d–d transitions could be measured. Analysis of the spectrum of **3** suggests the deep red colour is due to the overlap of the d–d transitions at around 520 nm and a broad intense band at 355 nm.

Some previous studies have suggested that the band at 350 nm was due to a charge transfer process.[9] However the similarity in the position of this band in both the nickel and the cobalt complexes **3** and **4**, suggests this assignment is erroneous. The transition can also be seen for the free ligand system when dissolved in acidic media.[18] The conclusion is that binding either metal or proton to the ring nitrogen leads to a shift in the intra-ligand band, and that this intense transition is ligand-based.

Magnetochemistry

Bulk magnetic susceptibility data were collected from polycrystalline samples of complexes **3** and **4**, under a constant magnetic field of 1 kG in the temperature range of 1.8 to 300 K. In Figs 2 and 3 are plots of the experimental data for **4** and **3**, respectively, in the form of both χ_m (magnetic susceptibility) or $\chi_m T$ *vs.* T, after correction for the diamagnetic contribution ($\chi_{dia} = -7.10$ and -6.74×10^{-4} cm^3 K mol^{-1} for **3** and **4**, respectively).

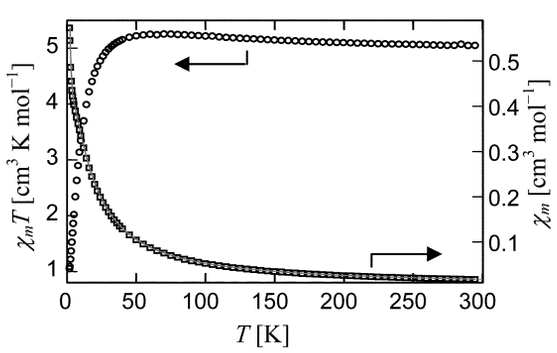

Fig. 2 Plots of experimental $\chi_m T$ *vs.* T (circles) and χ_m *vs.* T (squares) per molecule of **4**. The solid red line is a fit to the experimental values (see text for details).

The value of $\chi_m T$ at 300 K for the complex $[Ni_4(Mq)_4(piv)_4]$ **4** is 5.04 cm^3 K mol^{-1}, which corresponds to that of four magnetically uncoupled octahedral Ni^{II} centers with $^3A_2$ ground state and a calculated g term of 2.24. As the temperature is lowered, $\chi_m T$ experiences a very slight increase, reaching a maximum value of 5.26 cm^3 K mol^{-1} at 70 K, followed by a much sharper decline at lower temperatures, down to 1.05 cm^3 K mol^{-1} at 1.8 K.

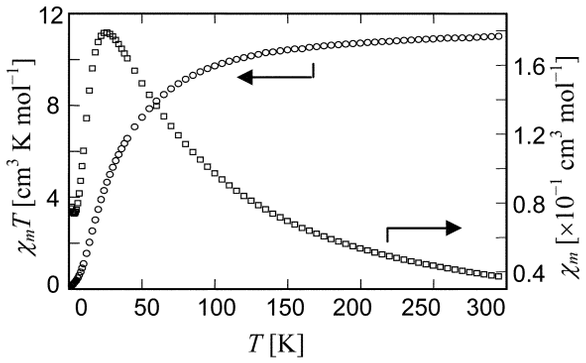

Fig. 3 Plots of experimental $\chi_m T$ *vs.* T (circles) and χ_m *vs.* T (squares) per molecule of **3**.

In order to quantify the nature of the magnetic exchange within the cluster, theoretical expressions of χ_m as a function of T were derived and fit to the experimental data. For this, a Heisenberg spin-Hamiltonian (eqn. (1)) was considered, where the idealized S_4 symmetry of the molecule was taken into account. Therefore two types of magnetic Ni ··· Ni interactions where included. As an approximation, zero field splitting (ZFS) parameters, usually small in this type of systems, were not included in the model, since this would have prevented us finding an analytical solution to this problem.

$$H = -2J_1(S_1S_3 + S_2S_4) - 2J_2(S_1S_2 + S_1S_4 + S_2S_3 + S_3S_4) \quad (1)$$

In the above Hamiltonian, S_i is the spin operator of the ith Ni^{II} center ($S_i = 2$), J_1 describes the interaction between the Ni^{II} ions bridged exclusively by the μ_3-alkoxide from the Mq ligands, J_2 corresponds to the exchange between Ni pairs bridged additionally by carboxylate ligands and the numbering scheme is as in Fig. 4. The energy values (eqn. (2)) and spin states of this

$$E(S_T,S_A,S_B) = -J_1[S_A(S_A + 1) + S_B(S_B + 1)] - J_2[S_T(S_T + 1) - S_A(S_A + 1) - S_B(S_B + 1)] \quad (2)$$

system were obtained by applying the Kambe vector coupling method,[19] using the transformations of spin angular momentum operators outlined in eqns. (3)–(5), as reported previously for other $[Ni^{II}_4]$ clusters with this symmetry.[17]

$$S_A = S_1 + S_3 \quad (3)$$

$$S_B = S_2 + S_4 \quad (4)$$

$$S_T = S_A + S_B \quad (5)$$

The spin states of the system, $|S_T,S_A,S_B\rangle$, and their corresponding energies, $E(S_T,S_A,S_B)$, as derived from the above relationships, were introduced into the Van Vleck equation in order to obtain the desired theoretical equation of $\chi_m = f(T)$. This function was fit to the experimental data (Fig. 2, solid line) through a least-squares procedure with g fixed at 2.24, to yield the following parameters; $J_1 = 3.4$ cm^{-1} and $J_2 = -1.1$ cm^{-1}. According to this result, complex **4** can be described as two weakly ferromagnetically coupled Ni_2 pairs that, in turn, are coupled antiferromagnetically *via* carboxylate bridges, leading to a diamagnetic spin ground state. The value J_1, however, is not in line with previous studies on $[Ni_4(OR)_4]^{4+}$ cubane clusters that show that for μ_3-alkoxide bridged Ni^{II}_2 pairs the interaction is antiferromagnetic if the average Ni–O–Ni angle is larger than 99° (102.5° in **4**).[20] The mean Ni–O–Ni angle for the pairs described by J_2 is 93.9°, thus, according to such studies the coupling is predicted to be ferromagnetic. The fact that the coupling within these pairs is antiferromagnetic can be explained by the presence of an additional carboxylate bridge in a *syn–syn* fashion, which favours the antiferromagnetic contribution to the coupling. The possibility for weak intermolecular interactions was allowed in a second fitting by including a mean-field correction term, $-zJ\langle S_{Tz}\rangle S_{Tz}$, in the Hamiltonian. This fit resulted in the overestimation of the intermolecular coupling over J_2. Moreover, the value obtained of J_1 was also deviated further from previous magneto-structural correlations on $[Ni^{II}_4]$ clusters. We therefore favour the first model over the second one.

The very small size of the exchange interactions creates a difficulty, in that J_2 is very close to the single ion anisotropy for a single Ni(II) centre. Therefore the value of J_2 should be treated with caution. As the ground state is $S = 0$, the zero-field splitting due to anisotropy will only contribute to the excited states. Therefore we believe the interpretation of the behaviour as due to two pairs of ferromagnetically coupled dimers that couple antiferromagnetically is sound; the values for the exchange interactions are less well determined.

The tetranuclear cobalt cluster $[Co_4(Mq)_4(piv)_4]$ **3** exhibits a value of $\chi_m T$ of 11.01 cm^3 K mol^{-1} at 300 K, which is higher than the spin-only value expected (7.5 cm^3 K mol^{-1}) for four uncoupled Co^{II} centers in the $^4T_1$ ground state (S = 3/2) with $g = 2$. This is because the orbital degeneracy of this state is not quenched and, consequently, there is a significant orbital contribution to the magnetic moment. For this reason, it is not possible to model the variable-temperature magnetic susceptibility and no attempt has been made to fit this data. As the temperature is lowered, $\chi_m T$ decreases to reach a value very close to zero (0.08 cm^3 K mol^{-1}) at 1.8 K. This behaviour indicates the presence of antiferromagnetic interactions between the metal centres within the molecule, as is obvious from the maximum observed in the plot of χ_m *vs.* T.

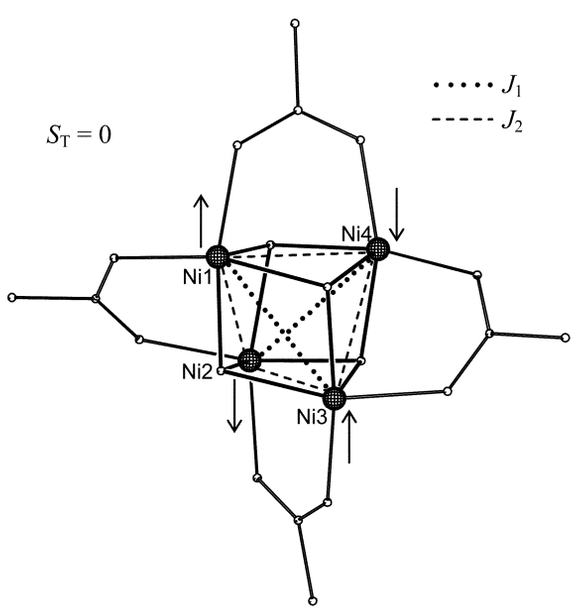

Fig. 4 Core representation of **4** showing the coupling scheme used in the magnetic model and the relative orientation of the Ni^{II} spins in the ground state. The pivalate ligands are also shown, without CH_3 groups.

Paramagnetic ^{1}H NMR

Compounds **3** and **4** were investigated by ^{1}H NMR in $CDCl_3$ solution. The coresponding spectra were strongly affected by the presence of the unpaired electrons of the paramagnetic ions. The ensuing electronic magnetic moment causes the broadening of the ^{1}H NMR resonances, which appear at abnormally large chemical shifts and prevent resolution of any hyperfine coupling.[21]

Table 5 300 MHz ^{1}H NMR data[a] for $[Ni_4(Mq)_4(piv)_4]$ (**4**) and $[Co_4(Mq)_4(piv)_4]$ (**3**)

Assignment (integ.)[b]	$[Ni_4(Mq)_4(piv)_4]$ (**4**)	$[Co_4(Mq)_4(piv)_4]$ (**3**)
piv (9)	5.30	61.05
Mq(CH_3) (3)	~ −1.7	~ −98.5
Mq(*ortho*) (1)	~ −17.6	~ 66.3
Mq (1 each)	−2.79, 16.17, 18.85, 53.64	−25.69, −24.21, −14.48, 36.38

[a] In $CDCl_3$, ppm. [b] Relative intensities.

The spectrum of **4** (Fig. 5(a), Table 5) spans a range of 60 to −20 ppm. It exhibits a set of seven broad resonances in the 1 : 1 : 1 : 1 : 1 : 3 : 9 intensity ratio. This shows the presence of one magnetically unique pivalate ligand (signal with intensity proportional to 9 at 5.30 ppm) and one Mq ligand. The fact that the signals are distributed on either side of the origin of chemical shifts is evidence that, for the Mq ligand, the coupling between the electronic and the nuclear magnetic moments is dominated by a π-delocalization mechanism. The two broadest signals of the spectrum correspond to the methyl group and to the proton in α with the alkoxide function of the Mq ligand (−1.7 and −17.16 ppm, respectively), since they are the closest to the paramagnetic centers (the broadness is proportional to r^{-6}, where r is the distance between the nuclear and the electronic magnetic dipoles). The individual assignment of the remainder of the signals could not be made. Therefore the spectrum of **4** is consistent with the retention of the solid-state structure and idealized symmetry of this complex in solution.

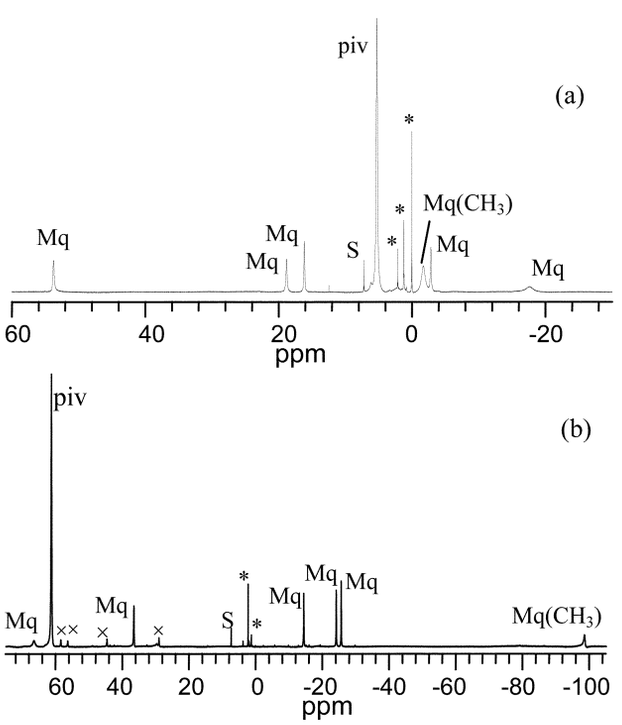

Fig. 5 300 MHz ^{1}H NMR spectra of (a) **4** and (b) **3** in $CDCl_3$ solution. Legend: piv, pivalate; Mq(CH_3), methyl from Mq; Mq, remaining protons of the Mq ligand; s, residual $CHCl_3$ from the solvent; '*', impurities from free pivalic acid or other solvents; '×', paramagnetic impurities (see text).

The ^{1}H NMR spectrum of **3** is shown in Fig. 5(b). The spectral window in this case is almost twice as wide as for **4**. Seven signals in the 1 : 1 : 1 : 1 : 1 : 3 : 9 intensity ratio dominate the spectrum (in addition to the peak from residual $CHCl_3$ of the solvent and a resonance from free pivalic acid). This is also explained by the existence of one magnetically unique pivalate and one Mq ligand. As with **4**, the peaks from pivalate, CH_3(Mq) and the proton next to the alkoxide group of Mq have been assigned (61.05, −98.5 and 66.3 ppm, respectively) based on their broadnesses and intensities. Unlike for the Ni compound, weaker signals from paramagnetic impurities are also observed. This is attributed to the existence of an equilibrium in solution, rather than impurity of the solid compound or degradation, as the same intensity ratio between the main set of signals and that of impurity peaks is maintained when the solution is kept for several days. The fact that the $[Co^{II}_4]$ compound is more labile than the corresponding $[Ni^{II}_4]$ cluster is consistent with the smaller crystal field stabilisation of cobalt(II) compared with nickel(II). Nevertheless, the spectrum in Fig. 5(b) is a strong indication that **3** is the predominant species present in solution.

Conclusions

A pair of tetranuclear cages has been made using hydroxyquinaldine ligands. The structures have a distorted cubane core. Magnetic studies show low spin ground states for both cages. NMR studies demonstrate the structures are maintained in solution.

References

1 M. A. Halcrow and G. Christou, *Chem. Rev.*, 1994, **94**, 2421.
2 R. H. Holm, *Adv. Inorg. Chem.*, 1992, **38**, 1.
3 G. Christou and J. B. Vincent, *ACS Symp. Ser.*, 1988, **372**, 238; R. Manchanda, G. W. Brudvig and R. H. Crabtree, *Coord. Chem. Rev.*, 1995, **144**, 1.
4 J. A. Bertland, C. Marbela and D. G. Vanderneer, *Inorg. Chim. Acta.*, 1978, **26**, 113.
5 J. K. Beattie, T. W. Hambley, J. A. Klepetko, A. F. Masters and P. Turner, *Polyhedron*, 1998, **17**, 1343.
6 E. Bouwmen, M. A. Bolcar, E. Libby, J. C. Huffman, K. Folting and G. Christou, *Inorg. Chem.*, 1992, **31**, 5185; N. K. Nagi, A. Harton, S. Donald, Y-S. Lee, M. Sabat, J. O'Conner and J. B. Vincent, *Inorg. Chem.*, 1995, **34**, 3813; Y. Kai, M. Morita, N. Yasuoka and N. Kasai, *Bull. Chem. Soc. Jpn.*, 1985, **58**, 6131; W. F. Weng, Y. S. Chen, M. Y. Chiang, S. S. Cher and C. P. Cheng, *Polyhedron*, 2002, **21**, 1081.
7 A. Yuchi, H. Murakami, M. Shiro, H. Wada and G. Nakagawa, *Bull. Chem. Soc. Jpn.*, 1992, **65**, 3362.
8 F. Jian, Y. Wang, L. Lu, X. Yang, X. Wang, S. Chantrapromma, H-K. Fun and I. A. Razak, *Acta. Crystallogr., Sect. C*, 2001, **57**, 714.
9 Y. Kushi and Q. Fernando, *J. Am. Chem. Soc.*, 1970, **92**, 91; H. Schmidbaur, J. Lettenbauer, O. Kumberger, J. Lachmann and G. Muller, *Z. Naturforsch., Tiel B*, 1991, **46**, 1065.
10 F. E. Mabbs, V. N. McLachlan, D. McFadden and A. T. McPhail, *J. Chem. Soc., Dalton Trans.*, 1973, 2016.
11 F. Franceschi, M. Guardigli, E. Solari, C. Floriani, A. Chiesi-Villa and C. Rizzoli, *Inorg. Chem.*, 1997, **36**, 4099; F. Franceschi, P. Fiaschi, A. Chiesi-Villa, C. Guastini and P. F. Zanazzi, *J. Chem. Soc., Dalton Trans.*, 1998, 1607.
12 M. Pasquali, P. Faischi, C. Floriani and P. F. Zanazzi, *Chem. Commun.*, 1983, 613.
13 G. Aromi, A. S. Batsanov, P. Christian, M. Helliwell, A. Parkin, S. Parsons, A. A. Smith, G. A. Timco and R. E. P. Winpenny, *Chem. Eur. J.*, in press.
14 J. Cosier and A. M. Glazer, *J. Appl. Crystallogr.*, 1986, **19**, 105.
15 SHELX-PC Package, Bruker Analytical X-ray Systems, Madison, WI, 1998.

16 R. A. Coxall, S. G. Harris, D. K. Henderson, S. Parsons, P. A. Tasker and R. E. P. Winpenny, *J. Chem. Soc., Dalton Trans.*, 2000, 2349.
17 M. A. Halcrow, J. S. Sun, J. C. Huffman and G. Christou, *Inorg. Chem.*, 1995, **34**, 4167.
18 J. P. Philips, W. H. Huber, J. W. Chung and L. L. Merritt, *J. Am. Chem. Soc.*, 1951, **73**, 630.
19 K. Kambe, *J. Phys. Soc. Jpn.*, 1950, **5**, 48.
20 J. H. Van Vleck, *The Theory of Electric, and Magnetic Susceptibilities*, Oxford University Press, Oxford, 1932.
21 M. W. Wemple, H. L. Tsai, K. Folting, D. N. Hendrickson and G. Christou, *Inorg. Chem.*, 1993, **32**, 2025.